

Isotherm and Thermodynamical Studies of Arsenic Adsorption from Water using Laterite

Ebenezer Annan¹, Daniel Amusah¹, Godfred Bright Hagan^{2*}, Augustine Nana Sekyi Appiah³

¹Department of Materials Science and Engineering, School of Physical and Mathematical Sciences, University of Ghana, Legon, Accra, Ghana.

²Department of Physics, School of Physical and Mathematical Sciences, University of Ghana, Legon, Accra, Ghana.

³Laboratory of Materials Research, Faculty of Mechanical Engineering, Silesian University of Technology, Gliwice, Poland.

*Corresponding author: gbhagan@ug.edu.gh

Abstract

This study investigates the removal of arsenic (As) from polluted water using laterite. Three different particle sizes 425, 850, and 106 μm of laterite were prepared, characterised and utilised as an adsorbent to remove As from polluted water. The highest removal efficiency was 94.90% and was associated with the particle size of 106 μm . The adsorption data can best be described by Langmuir Isotherm model, which had a superior *R*-square value of 0.99 to that of Freundlich adsorption model from the Isotherm modelling fitting. The results indicated that metal ion absorption occurs on a homogenous surface via monolayer adsorption and that the adsorption process may be controlled by chemisorption processes. The removal efficiency values were found to be increasing with increasing temperature. The enthalpy (ΔH°) and entropy (ΔS°) for the thermodynamical process at 308.15 K were 32.2 kJ/mol and 206.0 J/K mol, respectively, for the optimum particle size (106 μm) of the laterite. Gibb's Free Energy (ΔG°) was determined to be -31.70, -33.54, and -35.85 kJ/mol at temperatures 308.15, 318.15, and 328.15 K respectively. The negative ΔG° values reflect the feasibility and spontaneity of the adsorption process. The adsorption process can, thus, be described as endothermic. Lateritic soil adopted has a promising ability in arsenic adsorption.

Keywords: Laterite, arsenic removal, adsorption technology, thermodynamical modelling, temperature effect

Introduction

Anthropogenic sources such as mining wastes, petroleum refining, sewage sludge, agricultural chemicals, and ceramic industries play a major role in the pollution of our water bodies (Viraraghavan et al., 1999). Also, natural processes can serve as pollution sources. These include weathering, erosion of rocks, and volcanic emissions which produce pollutants into the environment. Some of these pollutants released into the water bodies largely contain heavy metals such as lead, cadmium, nickel, mercury as well as arsenic (Nagajyoti et al., 2010).

Arsenic is a naturally occurring substance present in rocks, water, air, animals, and plants. It is a kind

of metalloid that can exist in both inorganic and organic forms (Matschullat, 2000). In the presence of other elements such as iron and sulphur, arsenic species may be converted into various forms or turned into insoluble compounds (Mandal & Suzuki, 2002). Arsenic compounds are mostly odourless and colourless which create an elevated health risk. A previous publication reported that arsenic is a unique carcinogen. It is the only known human carcinogen for which there is adequate evidence of carcinogenic risk by both inhalation and ingestion (Kapaj et al., 2006). Research on the source, behaviour, and distribution of arsenic in the atmosphere, as well

as its removal technique, has been conducted around the world due to its high toxicity and widespread presence in the environment. High amounts of arsenic in water have been found in many countries, including parts of the United States, China, Chile, Bangladesh, Taiwan, Mexico, Argentina, Poland, Canada, Hungary, Ghana, and Japan (Chakraborti et al., 2002; Chen et al., 1994; He & Charlet, 2013; Karim, 2000; Ning, 2002; Smedley & Kinniburgh, 2002; Wang & Mulligan, 2006). Drinking water is considered as the major intake of arsenic compounds which increases the health risk of human life. Due to its health risks and difficulty in removal, the current recommended limit for arsenic in drinking water by the World Health Organization (WHO) is 0.01 mg/L.

Processes such as oxidation (Pierce & Moore, 1982; Sorlini & Gialdini, 2010), Co-precipitation (Choong et al., 2007; Kumar et al., 2004), ion exchange (Anirudhan & Unnithan, 2007), membrane technologies (Brandhuber & Amy, 2001), and adsorption are reported to remove arsenic from water. Many of these procedures are either expensive or not effective and sometimes difficult to carry out, but adsorption has been the most promising method to remove a more reasonable quantity of arsenic compounds from water compared to the other processes (Anirudhan & Unnithan, 2007; Choong et al., 2007; Kumar et al., 2004; Sorlini & Gialdini, 2010).

Many natural and synthetic sorptive media have been identified to dissolve arsenic, including activated alumina, activated carbon, iron, and manganese coated powder, kaolinite clay, hydrated ferric oxide, activated bauxite, titanium oxide, and selenium oxide (Brandhuber & Amy, 2001). In this research, lateritic soil is used due to their high iron oxide content.

It is estimated that over 140 million people have been exposed to drinking water containing more than 10 g/L of arsenic in recent decades (Bagchi, 2007). It has been established by WHO that long-term exposure to the metalloid element arsenic can cause cancer,

cardiovascular diseases, skin lesions as well as diabetes, and in the long run death. Arsenic is mainly found in water and food (Smith & Smith, 2004). While the effects of this poisonous agent are not readily visible, procedures to eliminate arsenic and have filtered water for use are being investigated. Cost-effective filtration systems have been developed to combat this arsenic contamination of water. However, these systems need expertise and prohibit easy use in developing countries due to socio-economic conditions that exist in such countries.

To address this challenge, adsorption technology, which uses raw materials and industrial waste in their natural or modified forms to remove arsenic from aqueous solutions is being explored. It is highly versatile and provides a cost-effective alternative to conventional chemical, physical remediation, and decontamination strategies (Mostafa et al., 2012). The nano-size, catalytic potential, large surface area, and high reactivity of adsorbents synthesised from local materials facilitate better arsenic removal efficiency. This research considers the use of the raw material, laterite as an adsorbent for arsenic removal. The study assesses the removal efficiency values of laterite as adsorbent and the effect of temperature on the removal efficiency of laterite along thermodynamical modelling.

Materials and Methods

Water samples was obtained from River Ankobra in the Wassa Amenfi East Municipal in the Western Region of Ghana. Figure 1 shows the geographical location of the river basin (Aduah et al., 2018).

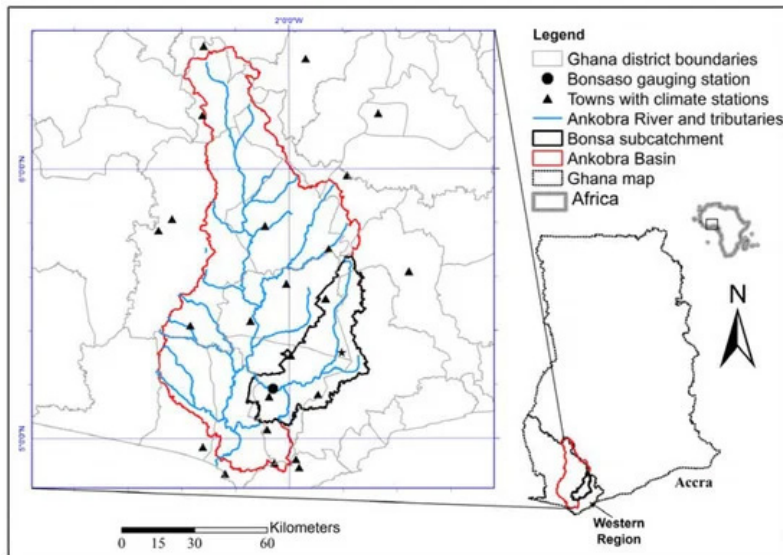


Fig. 1. Location of River Ankobra

The water samples were filtered using filter paper, frozen, and transported to the laboratory. Conc. nitric acid (16 N) was added to preserve the samples. The initial arsenic concentration in the samples was measured at the laboratory at the Ghana Standard Authority and compared to the levels after the absorption procedure.

Laterite Preparation and Characterisation

Samples of laterite soil were obtained from a road construction site at Amanfro on the Adentan-Dodowa road in the Greater Accra Region, Ghana. The laterite samples were stored in an oven at 100 °C for two hours. The samples were powdered using a mortar and pestle, and sieved into three particle sizes: 850 microns, 425 microns, and 106 microns (Figure 2)



(a)



(b)



(c)

Fig. 2. Preparation of laterite adsorbent: (a) Coarse laterite sampled from site (b) Sieving powdered laterite into different particle sizes (c) Weighing powdered laterite sample for batch adsorption studies

The characterisation of the laterite sample was carried out using X-ray powder diffraction (XRD), X-ray fluorescence (XRF), and Fourier Transform Infrared (FTIR). The FTIR analysis was performed using the Bruker Spectrum Two N™ (PerkinElmer, Frontier, Perkin Elmer, Ohio, USA) at laboratory of the Department of Chemistry, University of Ghana. 5 - 10 mg of the optimum particle size (106 µm) of the laterite was well compressed onto the diamond surface UATR holder of the FTIR device. The sample was scanned and ATR correction undertaken to normalise the spectrum output.

Batch Adsorption Experiment

Batch adsorption tests were performed on the polluted water sample to establish the adsorption removal efficiency ability for arsenic. A 100 mL of the polluted water sample was thoroughly mixed with a specified dosage of the adsorbent in a 250 mL flask. To ensure thorough mixing, the mixture was positioned in an orbital shaker (at a constant rate of 200 rpm) for the required contact time. The pH of the sample was measured. The mixture was then filtered, and 20 mL of the filtrate was used in determining the concentration of arsenic in the solution. Different adsorption processes were carried out to ascertain the effect of adsorption dosage, contact time, and temperature. The volume of the solution (V) was maintained throughout the experiment.

To explore the effect of adsorbent dosage on removal efficiency, various lateritic dosage (1.0 - 3.5 mg in the

intervals of 0.5 mg) for the particle sizes 106, 450, and 850 µm were used. A 100 mL arsenic solution was added to each mass of adsorbent, and the mixture was agitated on a mechanical shaker spinning at 200 rpm for a maximum contact duration of 60 min.

The effect of time on removal was also investigated for the various particle sizes at optimum dosage (from 30 to 270 min at 30 min intervals). The concentration of arsenic was determined. The effect of temperature on removal of arsenic from polluted water was carried out at 35, 45, and 55 °C for the particle size that showed best removal efficiency.

Isotherm Modelling of Adsorption Data

Freundlich and Langmuir models are the basic models adopted in this research for isothermal process modelling. The Langmuir equation assumes that the maximum adsorption takes place when the surface is covered by adsorbate in a monolayer and that the point of valance exists on the surface of the adsorbent and that each of these sites (with equal affinity and independent) are capable of adsorbing one molecule. The Freundlich model is empirical.

The original and linear forms of the Langmuir and Freundlich models are given by equations (1) and (2), respectively.

Original Form

$$q_e = \frac{q_m \times K_L \times C_e}{1 + K_L \times C_e}$$

$$q_e = K_F \times C_e^{1/n}$$

Linear Form

$$\frac{C_e}{q_e} = \frac{1}{K_L q_m} + \frac{1}{q_m} C_e \quad (1)$$

$$\log q_e = \log K_F + \frac{1}{n} \log C_e \quad (2)$$

where K_L and q_m are the Langmuir constant and maximum adsorption capacity (mg/g) respectively; q_e is the adsorption capacity (mg/g) at equilibrium; K_F and $(1/n)$ are the Freundlich constants; and C_e is the equilibrium concentration (mg/L).

Thermodynamical Modelling

Thermodynamic parameters, including Gibbs free energy change (ΔG°), enthalpy change (ΔH°) and entropy change (ΔS°) serve to evaluate the effect of temperature on the adsorption of arsenic onto adsorbents and provide in-depth information regarding the inherent energy changes associated with the adsorption process (Chen & Zhang, 2014). These parameters are calculated from equations (3) – (5):

$$\Delta G^\circ = -RT \ln K_L^\circ \quad (3)$$

where R is the universal gas constant (8.314 J/mol K), T the temperature (K), and K_L° the (dimensionless) ‘thermodynamic’ Langmuir constant for the adsorption process.

$$\ln K_L^\circ = (\Delta S^\circ/R) - (\Delta H^\circ/RT) \quad (4)$$

$$\Delta G^\circ = \Delta H^\circ - T\Delta S^\circ \quad (5)$$

RESULTS AND DISCUSSION

Characterisation

Figure 3a displays the FTIR spectra from 4000 to 500 cm^{-1} of the lateritic soil while Figure 3b depicts the XRD pattern of laterite.

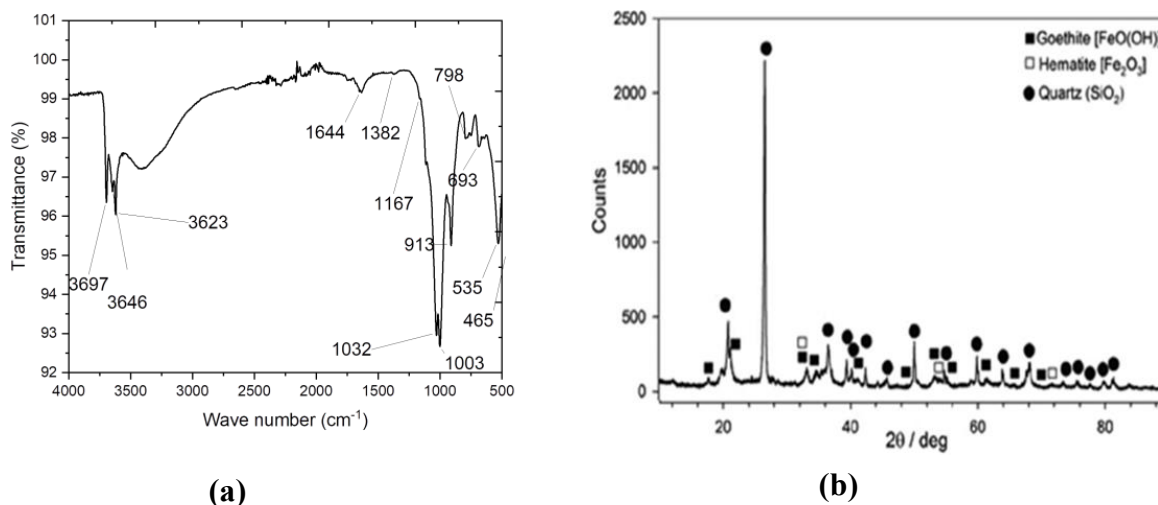


Fig. 3. (a): FTIR spectrum for laterite (b): Xray-diffraction patterns of laterite soil adsorbent

From Figure 3a, the band between 3697 and 3646 cm^{-1} was allocated to the $-\text{OH}$, Si, and Al groups. Water molecules were allocated to the 1644 cm^{-1} frequency band. The spectra showed bands at 1032, 1003, and 913 cm^{-1} due to the existence of Si–O–Fe, Al–OH, and Fe–OH vibrations, respectively. Laterite’s hematite structure led to the Fe–O bonds extending at 535 cm^{-1} and 465 cm^{-1} of the spectra (Maiti et al., 2013). The most

common phases were quartz (SiO_2), hematite (Fe_2O_3), and goethite ($\text{FeO}(\text{OH})$) (Figure 3b). At extremely low intensity, several peaks suggested Al_2O_3 . The laterite mineralogical phases utilised in this investigation are similar to laterite used in other studies (Forster et al., 2016).

Table 1 shows the band peaks and its respective chemical compounds found on the FTIR graph, whereas Table 2 gives the various percentages for the major oxides in the adsorbent.

Table 1: Classification of FTIR peaks

Wavenumber (cm ⁻¹)	Absorption range (cm ⁻¹)	Appearance	Group	Compound class
3697, 3646, 3623	3700 - 3584	Medium, Sharp	O-H stretching	Free alcohol
1644	1648 - 1638	Strong	C=C stretching	Monosubstituted alkene
1382	1385 - 1380	Medium	C-H bending	Gem dimethyl alkane
1167	1205 - 1124	Strong	C-O stretching	Secondary alcohol
1032	1070 - 1030	Strong	S=O stretching	Sulfoxide
913	915 - 905	Strong	C=C bending	Monosubstituted alkene
798	840 - 790	Medium	C=C bending	Trisubstituted alkene
693	730 - 665	Strong	C=C bending	Disubstituted (cis) alkene
535	600 - 500	Strong	C-I stretching	Halo compound

Table 2: Chemical constituents of laterite

Major Oxide	Value (%)
Al ₂ O ₃	15.0
Fe ₂ O ₃	40.1
SiO ₂	33.2
MnO ₂	0.7
P ₂ O ₅	0.5
Na ₂ O ₃	-
K ₂ O ₃	0.8
CaO	-

Effect of Adsorbent Dosage on Removal Efficiency

The impact of laterite dosage on arsenic removal was investigated using varied masses of laterite adsorbent (1.0, 1.5, 2.0, 2.5, 3.0, and 3.5 mg) (Figure 4a). The removal efficiency for the optimum dosage, (3.5 mg) was determined by leaving it in contact with arsenic-contaminated water for 270 min and collecting a sample every 30 min (Figure 4b).

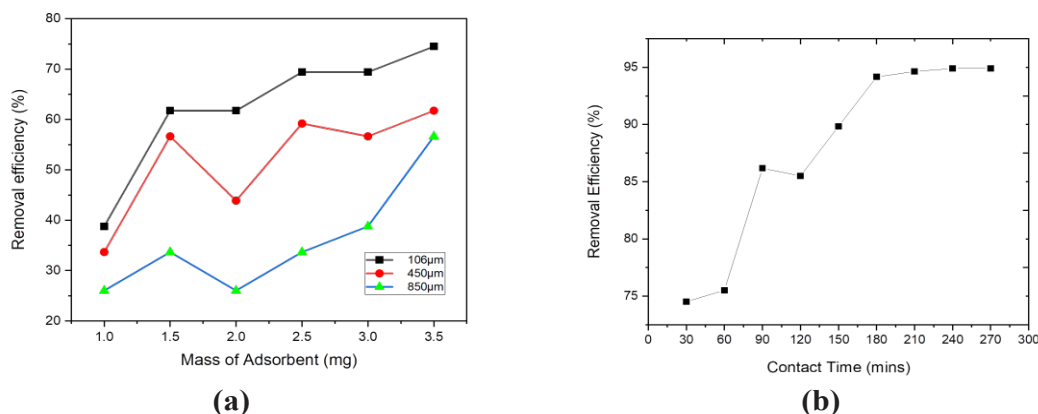


Fig. 4. (a) Effects of laterite dosage on arsenic removal efficiency
(b) Effect of contact time on adsorption of arsenic for optimum dosage

The concentration of the arsenic solution was kept constant at 0.0392 mg/L, while the volume was also kept constant at 100 mL. The removal effectiveness of the adsorbent rose with increasing adsorbent mass and with a decrease in particle size (Figure 4a). Thus, as the dosage of adsorbent increases, the removal efficiency increases, proving that the mass of adsorbent is directly proportional to removal efficiency (Mackenzie et al., 1979). Adsorption of arsenic from water proceeds in two stages: the first being a rapid formation of a monolayer, followed by a steady plateau sorption process (Mondal et al., 2008). This phenomenon explains the observation of rapid increase in the removal efficiency as the adsorbent dosage was gradually increased, followed by a steady rise in the removal efficiency until equilibrium was obtained. The number of active sites, surface area, and pores available for mass transfer also influenced the observation of higher removal efficiency as the dosage of adsorbent increased (Saadon et al., 2018). The effects of adsorbent dosage observed in this study are similar to those of other studies (Biltayib et al., 2021; Hassani et al., 2014; Padmavathy et al., 2016) that have reported that an increase in the adsorbent dosage over an optimum dose proceeds with a slow increase in the removal efficiency to a maximum value. Therefore, as the adsorbent dosage gets increased over the desired value, there is no significant impact on the sorption percentage of arsenic

(Aryal et al., 2010). Increasing the adsorbent dosage over the optimum value also results in unsaturation of some binding sites, creating a limitation of arsenic mobility (Roy et al., 2013).

The change in contact time behaviour for a constant mass (the optimal dosage of 3.5 mg) is illustrated in Figure 4b. The removal efficiency recorded for the first 30 min was 74.52%. This increased up to the 90-min mark and it decreased for the next 30 minutes. The removal efficiency then increased steadily up to the 180-min mark at 94.90% and remained at equilibrium. This can be explained as follows: as adsorption process proceeds, the fixed adsorbent active sites get filled with the arsenic thereby decreasing the number of active sites available; at saturation point all the active sites get filled up and hence the rate of removal of arsenic stays at equilibrium (Mohammed et al., 2015). Similar observations are reported by other time-dependent adsorption research (Chen et al., 2011; Jiang et al., 2018; Zhang et al., 2013), presenting the most significant reason as the availability of empty internal and surface pores that get occupied by the adsorbate molecules as time progresses until reaching equilibrium (Olatunji et al., 2015). The removal effectiveness of arsenic by the laterite adsorbent improved with the increased contact time, according to the overall findings of the study.

Effect of Adsorbent Particle Size

As the mass of adsorbent increased with the varied particle sizes (106, 450, and 850 μm), the removal efficiency increased. The removal efficiency for 106 μm adsorbent size improved from 38.7 to 74.5%, while 450 μm particle size grew from 33.7 to 61.7%, and 850 μm particle size increased from 26 to 56% within the same time interval. The optimum removal effectiveness for the six masses employed in the adsorption tests occurred with 3.5 mg of the 106 μm laterite, with an average removal efficiency of 74.5% (Figure 4a). However, the removal efficiency increased to 94.90% at a contact time of 270 min (Figure 4b). Adsorbents with relatively smaller particle sizes have larger surface area. Coupled with the material's intrinsic properties of crystallinity and porosity, transport of adsorbates during the sorption process is facilitated. Particle size significantly affects the removal efficiency, as well as the adsorption capacity. The smaller the particle size, the faster the rate of adsorption, and hence the better the removal efficiency. In a study by Yusof *et al.* (2020), palm oil fuel ash (POFA) powder was used as adsorbent for removal of As(II) and As(V) from water, with a wide range of particle sizes between 30 and 125 μm . It was observed that when the smallest

particle size of 30 μm was used, the maximum removal efficiency of 40 and 50% of As(II) and As(V) were obtained, respectively. Similarly, this observation is consistent with other studies (Huang et al., 2020; Kumar et al., 2019; Yi et al., 2020) which have reported that smaller particle sizes increase good contact between the adsorbate and the adsorbent, eventually increasing the removal efficiency and adsorption capacity (Aljeboree et al., 2017). The reduction in the removal efficiency as the particle size was increased in this study can therefore be attributed to the reduction in the surface area, thus fewer active sites on the laterite adsorbents to interact with the arsenic adsorbate.

Isotherm Modelling of Adsorption Data

Langmuir and Freundlich's isotherm models are utilised to explain the processes of arsenic ion adsorption onto laterite. Langmuir and Freundlich isotherm experiments were carried out to determine the maximum adsorption capacity of laterite adsorbent towards arsenic. The linearized form of the Langmuir isotherm model is provided in equation (1) with fitting plot shown in Figure 5a.

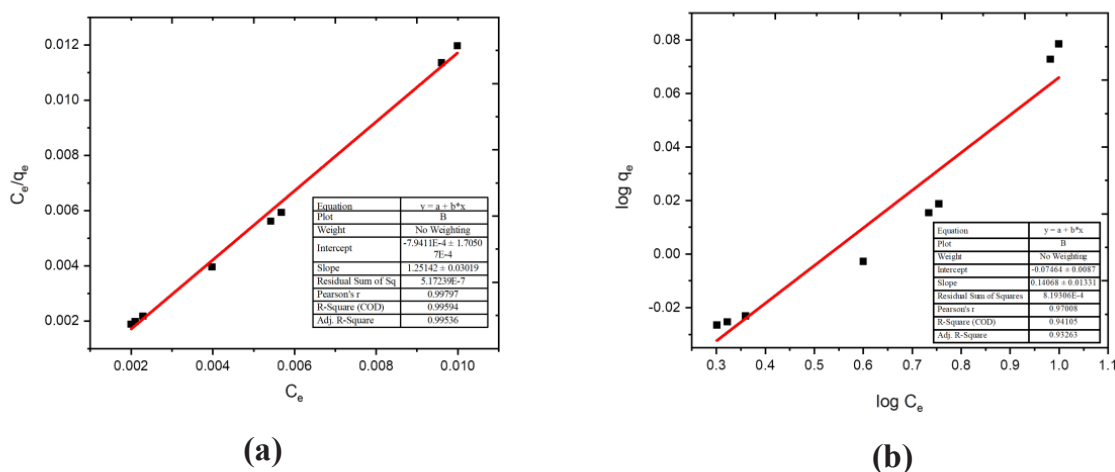


Fig. 5. (a) Langmuir Isotherm Model of the experimental data

(b) Freundlich Isotherm model fit of adsorption data

The adsorption constants of Langmuir isotherm model parameters, q_{max} and K_L , were estimated via the fitting plot from equation (1) and obtained as 0.799 mg/L and 1564.24 L/mg, respectively. The correlation coefficient of Langmuir isotherm (R^2) was 0.995 (Figure 5a), depicting a linear relationship between the plotted parameters (with R^2 value approximately 1). For an adsorption to obey the Langmuir isotherm model, a dimensionless factor, R_L must be satisfied. This factor is related to K_L and the initial concentration of adsorbate, C_o according to equation (6).

$$R_L = \frac{1}{1 + K_L \times C_o} \quad (6)$$

The nature of adsorption is indicated by the value of R_L ; for $R_L < 1$, adsorption is favorable; for >1 , adsorption is unfavorable; for $R_L = 1$, adsorption is linear (Maji et al., 2008). The computed value of R_L from this study is 0.24, indicating a favorable adsorption. Thus, it was observed that the adsorption of arsenic onto laterite adsorbent

correlated well with the Langmuir equation. Among the implications is that, metal ion adsorption occurs on a homogeneous monolayer surface adsorption with no interaction between the adsorbed ions.

All surface sites are identical and can only accommodate one adsorbed molecule; a molecule's ability to be adsorbed on a given site is independent of its neighbouring site occupancy; adsorption is reversible, and the adsorbed molecule cannot migrate across the surface or interact with neighbouring molecules (Anah & Astrini, 2018).

The linear fit for the Freundlich model is shown in Figure 5b. According to equation (2), the Freundlich isotherm model parameters: adsorption capacity, K_F , and adsorption intensity index, n , are determined to be 0.842 and 7.107, respectively (Table 3). The correlation coefficient (R^2) for the Freundlich isotherm plot was 0.941 (Figure 5b). A summary of the Langmuir and Freundlich isotherm model parameters are presented in Table 3 from this study.

Table 3: Isotherm model parameters for Laterite adsorbent

Langmuir Adsorption Model				Freundlich Adsorption Model			
Adsorbent (mg)	K_L (L/mg)	q_{max} (mg/L)	R^2	Adsorbent Usage (mg)	K_F (L/mg)	n	R^2
3.5	1564.24	0.79911	0.9959	3.5	0.84217	7.10732	0.9411

Effect of Temperature on Arsenic adsorption

Figure 6 depicts the contact time behaviour at constant mass with temperature variation for the 106 μm adsorbent.

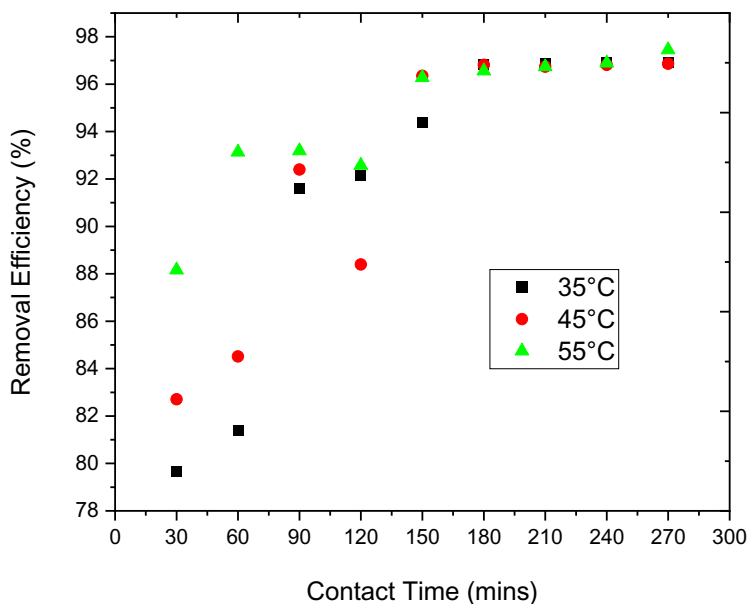


Fig. 6. Graph showing the effect of Temperature on adsorption

At a temperature of 35 °C and a constant mass of 3.5 mg for 30 min, the removal efficiency improves to 79.67% until it equilibrates at 96.94% roughly after 180 minutes. At a temperature of 45 °C and a constant mass of 3.5 mg, the removal effectiveness rises to 82.70% until it reaches 96.86% after 150 min of continuous arsenic adsorption. At a temperature of 55 °C and a constant mass of 3.5 mg, the removal efficiency rises from 88.16 to 97.45% after 180 min of continuous removal.

It was observed that when the temperature increased, the adsorbent's removal effectiveness improved. As the temperature rises, the mobility of ions or molecules in the flowing water accelerates, resulting in greater kinetic energy. As a result, the migration rate of arsenic ions onto the adsorbent's surface increased, increasing the adsorbent's adsorption capacity for arsenic ions. Other

studies (Mohapatra et al., 2007) have shown, however, that a contrast observation in the removal efficiency is observed when the temperature is further increased. At higher temperatures, there is instability of the adsorbent-adsorbate complex, resulting in an escape of the adsorbed adsorbates from the adsorbent into the bulk solution. This unstable complex can also cause damage to the active sites of the adsorbents resulting in a decline in the adsorptive capacity and removal efficiency (Mohapatra et al., 2007).

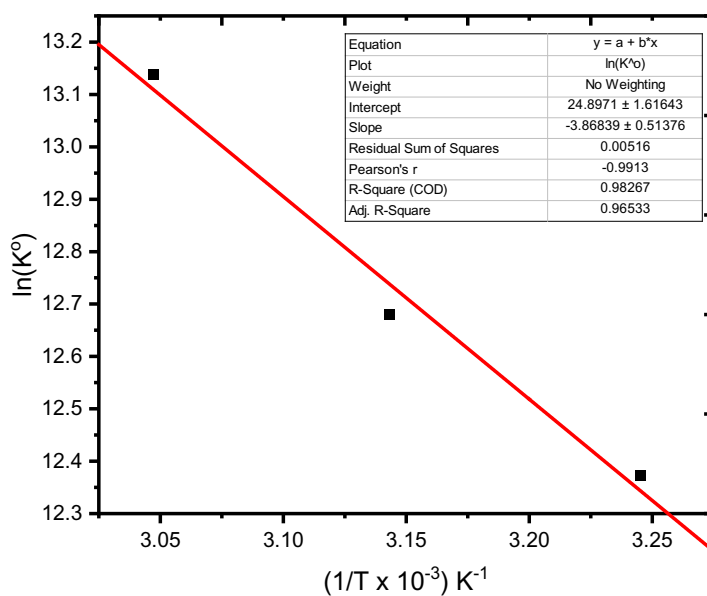


Fig. 7. Van't Hoff plot for thermodynamical studies

Thermodynamical Modelling

The Van't Hoff graph (Figure 7) which is a natural logarithm of K° ($\log K^\circ$) versus the reciprocal of the temperature ($1/T$) was first plotted. The thermodynamical parameters, enthalpy (ΔH°) and entropy (ΔS°) parameters were estimated from equations (3) and (4).

The values of Gibb's free energy ΔG° (kJ/mol) were calculated from ΔH° and ΔS° (Table 4). The Van't Hoff plot indicates an endothermic adsorption process with the negative ΔG° values confirming the feasibility and spontaneity of the adsorption process.

Table 4: Thermodynamical Parameters for arsenic adsorption onto 106 μm Lateritic soil

Temperature T (K)	K_L (L/mg)	K_L° ($\times 10^5$)	$\ln K_L^\circ$	ΔG° (KJ/mol)	ΔH° (KJ/mol)	ΔS° (J/K mol)
308.15	3151.13	2.3608	12.37	-31.70	32.16	206.0
318.15	4285.60	3.2108	12.67	-33.54		
328.15	6785.01	5.0833	13.14	-35.85		

Conclusion and Recommendations

The goal of this study was to identify and synthesise low-cost adsorbents from locally available materials that have the potential to remove arsenic from water. The concentration of arsenic in river Ankobra was determined and batch adsorption adopted for the experiment. For the adsorption data, isotherm modelling, and effect of temperature were studied.

Laterite was prepared as an adsorbent for the removal of arsenic from polluted water in Ghana. Arsenic was removed from polluted water using the lateritic adsorbent at three different particles sizes. The laterite with the smallest particle size (106 μm) at a contact time of 270 min exhibited the best removal efficiency of 94.90 percent and the maximum adsorptive capacity of 1.063 mg/g. It was observed that as the temperature of the solution increased, adsorption is more efficient. The adsorption process was well-suited to the Langmuir isotherm model. The results indicate that metal ion absorption occurs on a homogenous surface via monolayer adsorption.

Further work would consider BET and SEM of the laterite sample. The determination of the surface area via BET and the phases via SEM of the particles will help explain the mechanism of the removal of arsenic by laterite. Additionally, composites with nanoparticles can be explored to enhance the removal efficiency of laterite. It is anticipated that these further works could produce a maximum adsorptive capacity for laterite that would compare with the 6.75 mg/g value obtained for red mud (Chakraborti et al., 2002).

Acknowledgement

The authors would like to acknowledge the insightful contributions from Associate Professor Emmanuel Nyankson and Mr. David Adebem Anafo of the Department of Materials Science and Engineering, University of Ghana. The contribution of Mr. Samuel Owusu-Atuah of the Department of Chemistry, University of Ghana, with the FTIR analysis is also duly acknowledged.

References

- Aduah, M. S., Jewitt, G. P., & Toucher, M. L. (2018). Assessing impacts of land use changes on the hydrology of a lowland rainforest catchment in Ghana, West Africa. *Water*, 10(1), 9.
- Aljeboree, A. M., Alshirifi, A. N., & Alkaim, A. F. (2017). Kinetics and equilibrium study for the adsorption of textile dyes on coconut shell activated carbon. *Arabian journal of chemistry*, 10, S3381-S3393.
- Anah, L., & Astrini, N. (2018). Isotherm adsorption studies of Ni (II) ion removal from aqueous solutions by modified carboxymethyl cellulose hydrogel. IOP Conference Series: Earth and Environmental Science,
- Anirudhan, T., & Unnithan, M. R. (2007). Arsenic (V) removal from aqueous solutions using an anion exchanger derived from coconut coir pith and its recovery. *Chemosphere*, 66(1), 60-66.
- Aryal, M., Ziaqova, M., & Liakopoulou-Kyriakides, M. (2010). Study on arsenic biosorption using Fe (III)-treated biomass of *Staphylococcus xylosus*. *Chemical Engineering Journal*, 162(1), 178-185.
- Bagchi, S. (2007). Arsenic threat reaching global dimensions. In: Can Med Assoc.
- Biltayib, B. M., Bonyani, M., Khan, A., Su, C.-H., & Yu, Y.-Y. (2021). Predictive modeling and simulation of wastewater treatment process using nano-based materials: Effect of pH and adsorbent dosage. *Journal of Molecular Liquids*, 343, 117611.
- Brandhuber, P., & Amy, G. (2001). Arsenic removal by a charged ultrafiltration membrane—influences of membrane operating conditions and water quality on arsenic rejection. *Desalination*, 140(1), 1-14.
- Chakraborti, D., Rahman, M. M., Paul, K., Chowdhury, U. K., Sengupta, M. K., Lodh, D., Chanda, C. R., Saha, K. C., & Mukherjee, S. C. (2002). Arsenic calamity in the Indian subcontinent: what lessons have been learned? *Talanta*, 58(1), 3-22.
- Chen, S.-L., Dzeng, S. R., Yang, M.-H., Chiu, K.-H., Shieh, G.-M., Wai, C. M., & technology. (1994). Arsenic species in groundwaters of the blackfoot

- disease area, Taiwan. *Environmental science*, 28(5), 877-881.
- Chen, Y.-G., Ye, W.-M., Yang, X.-M., Deng, F.-Y., & He, Y. J. E. E. S. (2011). Effect of contact time, pH, and ionic strength on Cd (II) adsorption from aqueous solution onto bentonite from Gaomiaozhi, China. *Environmental Earth Sciences*, 64(2), 329-336.
- Chen, Y., & Zhang, D. (2014). Adsorption kinetics, isotherm and thermodynamics studies of flavones from *Vaccinium Bracteatum* Thunb leaves on NKA-2 resin. *Chemical Engineering Journal*, 254, 579-585.
- Choong, T. S., Chuah, T., Robiah, Y., Koay, F. G., & Azni, I. (2007). Arsenic toxicity, health hazards and removal techniques from water: an overview. *Desalination*, 217(1-3), 139-166.
- Forster, J., Pickles, C., & Elliott, R. J. M. E. (2016). Microwave carbothermic reduction roasting of a low grade nickeliferous silicate laterite ore. 88, 18-27.
- Hassani, A., Alidokht, L., Khataee, A., & Karaca, S. (2014). Optimization of comparative removal of two structurally different basic dyes using coal as a low-cost and available adsorbent. *Journal of the Taiwan Institute of Chemical Engineers*, 45(4), 1597-1607.
- He, J., & Charlet, L. (2013). A review of arsenic presence in China drinking water. *Journal of hydrology*, 492, 79-88.
- Huang, B., Yuan, Z., Li, D., Zheng, M., Nie, X., Liao, Y., & Impacts. (2020). Effects of soil particle size on the adsorption, distribution, and migration behaviors of heavy metal (loid) s in soil: a review. *Environmental Science: Processes*, 22(8), 1596-1615.
- Jiang, J., Li, W., Zhang, X., Liu, J., & Zhu, X. (2018). A new approach to controlling halogenated DBPs by GAC adsorption of aromatic intermediates from chlorine disinfection: effects of bromide and contact time. *Separation Purification Technology*, 203, 260-267.
- Kapaj, S., Peterson, H., Liber, K., & Bhattacharya, P. (2006). Human health effects from chronic arsenic poisoning—a review. *Journal of Environmental Science Health, Part A*, 41(10), 2399-2428.
- Karim, M. M. (2000). Arsenic in groundwater and health problems in Bangladesh. *Water Research*, 34(1), 304-310.
- Kumar, P. R., Chaudhari, S., Khilar, K. C., & Mahajan, S. P. (2004). Removal of arsenic from water by electrocoagulation. *Chemosphere*, 55(9), 1245-1252.
- Kumar, P. S., Korving, L., Keesman, K. J., van Loosdrecht, M. C., & Witkamp, G.-J. (2019). Effect of pore size distribution and particle size of porous metal oxides on phosphate adsorption capacity and kinetics. *Chemical Engineering Journal*, 358, 160-169.
- Mackenzie, F. T., Lantzy, R. J., & Paterson, V. (1979). Global trace metal cycles and predictions. *Journal of the International Association for Mathematical Geology*, 11(2), 99-142.
- Maiti, A., Thakur, B. K., Basu, J. K., & De, S. (2013). Comparison of treated laterite as arsenic adsorbent from different locations and performance of best filter under field conditions. *Journal of Hazardous materials*, 262, 1176-1186.
- Maji, S. K., Pal, A., & Pal, T. (2008). Arsenic removal from real-life groundwater by adsorption on laterite soil. *Journal of Hazardous materials*, 151(2-3), 811-820.
- Mandal, B. K., & Suzuki, K. T. (2002). Arsenic round the world: a review. *Talanta*, 58(1), 201-235.
- Matschullat, J. (2000). Arsenic in the geosphere—a review. 249(1-3), 297-312.
- Mohammed, J., Nasri, N. S., Zaini, M. A. A., Hamza, U. D., & Ani, F. N. (2015). Adsorption of benzene and toluene onto KOH activated coconut shell based carbon treated with NH₃. *International Biodeterioration Biodegradation*, 102, 245-255.

- Mohapatra, D., Mishra, D., Chaudhury, G. R., & Das, R. P. (2007). Arsenic adsorption mechanism on clay minerals and its dependence on temperature. *Korean Journal of Chemical Engineering*, 24(3), 426-430.
- Mondal, P., Majumder, C., & Mohanty, B. (2008). Effects of adsorbent dose, its particle size and initial arsenic concentration on the removal of arsenic, iron and manganese from simulated ground water by Fe³⁺ impregnated activated carbon. *Journal of Hazardous materials*, 150(3), 695-702.
- Mostafa, M., & Hoinkis, J. (2012). Nanoparticle adsorbents for arsenic removal from drinking water: a review. *Journal of Environmental Science Health, Management Engineering Research*, 1(1), 20-31.
- Nagajyoti, P. C., Lee, K. D., & Sreekanth, T. (2010). Heavy metals, occurrence and toxicity for plants: a review. *Environmental chemistry letters*, 8(3), 199-216.
- Ning, R. Y. (2002). Arsenic removal by reverse osmosis. *Desalination*, 143(3), 237-241.
- Olatunji, M. A., Khandaker, M. U., Mahmud, H. E., & Amin, Y. M. (2015). Influence of adsorption parameters on cesium uptake from aqueous solutions—a brief review. *RSC advances*, 5(88), 71658-71683.
- Padmavathy, K., Madhu, G., & Haseena, P. (2016). A study on effects of pH, adsorbent dosage, time, initial concentration and adsorption isotherm study for the removal of hexavalent chromium (Cr (VI)) from wastewater by magnetite nanoparticles. *Procedia Technology*, 24, 585-594.
- Pierce, M. L., & Moore, C. B. (1982). Adsorption of arsenite and arsenate on amorphous iron hydroxide. *Water Research*, 16(7), 1247-1253.
- Roy, P., Mondal, N. K., Bhattacharya, S., Das, B., & Das, K. (2013). Removal of arsenic (III) and arsenic (V) on chemically modified low-cost adsorbent: batch and column operations. *Applied Water Science*, 3(1), 293-309.
- Saadon, S. A., Yunus, S. M., Yusoff, A. R., Yusop, Z., Azman, S., Uy, D., & Syafiuddin, A. (2018). Heated laterite as a low-cost adsorbent for arsenic removal from aqueous solution. *Malaysian Journal of Fundamental Applied Sciences*, 14(1), 1-8.
- Smedley, P. L., & Kinniburgh, D. G. (2002). A review of the source, behaviour and distribution of arsenic in natural waters. *Applied geochemistry*, 17(5), 517-568.
- Smith, A. H., & Smith, M. M. H. (2004). Arsenic drinking water regulations in developing countries with extensive exposure. *Toxicology*, 198(1-3), 39-44.
- Sorlini, S., & Gialdini, F. (2010). Conventional oxidation treatments for the removal of arsenic with chlorine dioxide, hypochlorite, potassium permanganate and monochloramine. *Water Research*, 44(19), 5653-5659.
- Viraraghavan, T., Subramanian, K., & Aruldoss, J. (1999). Arsenic in drinking water—problems and solutions. *Water Science and Technology*, 40(2), 69-76.
- Wang, S., & Mulligan, C. N. (2006). Occurrence of arsenic contamination in Canada: sources, behavior and distribution. *Science of the total Environment*, 366(2-3), 701-721.
- Yi, M., Cheng, Y., Wang, Z., Wang, C., Hu, B., & He, X. (2020). Effect of particle size and adsorption equilibrium time on pore structure characterization in low pressure N₂ adsorption of coal: An experimental study. *Advanced Powder Technology*, 31(10), 4275-4281.
- Yusof, M. S. M., Othman, M. H. D., Wahab, R. A., Jumbri, K., Razak, F. I. A., Kurniawan, T. A., Samah, R. A., Mustafa, A., Rahman, M. A., & Jaafar, J. (2020). Arsenic adsorption mechanism on palm oil fuel ash (POFA) powder suspension. *Journal of Hazardous materials*, 383, 121214.
- Zhang, J., Cai, D., Zhang, G., Cai, C., Zhang, C., Qiu, G., Zheng, K., & Wu, Z. (2013). Adsorption of methylene blue from aqueous solution onto multiporous palygorskite modified by ion beam bombardment: Effect of contact time, temperature, pH and ionic strength. *Applied Clay Science*, 83, 137-143.